

BEYOND LAYERS: A GLOBAL MESSAGE-PASSING MECHANISM FOR HETEROPHILIC GRAPHS

Anonymous authors

Paper under double-blind review

ABSTRACT

The effectiveness of most graph neural networks is largely attributed to the message-passing mechanism. Despite the significant success in homophilic graphs (*i.e.*, similar nodes are connected by edges), message-passing mechanism in heterophilic graphs (*i.e.*, dissimilar nodes are connected by edges) is still challenging. Due to the existence of low-order but dissimilar neighbor nodes in a path, messages from similar but high-order neighbor nodes are often weakened. In this paper, firstly, we conduct both theoretical and empirical analysis of the layer-by-layer local nature of the message-passing mechanism. Then, we propose a novel GloMP-GNN for heterophilic graphs by comprehensively introducing global insights into the message-passing mechanism. 1) During the message propagation phase, the global insight is introduced from the perspective of graph structure. We design a structure-based global propagation strategy, where messages can be effectively propagated with the bridge of virtual edges between a global virtual node and graph nodes. Moreover, a global edge adaption approach is included to aggregate messages with adaptive edge weight adjustment. 2) During the feature updating phase, the global insight is introduced with a feature-augmented compensatory updating method. Through a multi-view feature updating mechanism, the node feature representation can be effectively augmented by compensating the weakened message from different views. Finally, we conduct extensive experimental evaluations on eight datasets, which demonstrate the superiority of our proposed GloMP-GNN. As broader impacts, GloMP-GNN consistently performs well across multiple layers and also effectively prevents the over-smoothing problem. Codes are available on Github¹.

1 INTRODUCTION

Graph Neural Network (GNN) has emerged as an important method for graph representation learning, which have been widely used across various fields, such as social network analysis Huang et al. (2024); Yang et al. (2022), bioinformatics Zhang et al. (2024); Liu et al. (2024), and financial risk assessment Wang et al. (2023); Qian et al. (2024). The effectiveness of most GNNs is largely attributed to the message-passing mechanism Gilmer et al. (2017a), a prevalent paradigm that aggregates information from neighbor nodes to update the representation of nodes. Despite the significant success in homophilic graphs (*i.e.*, similar nodes are connected by edges), message-passing mechanism in heterophilic graphs (*i.e.*, dissimilar nodes are connected by edges) is still challenging. Due to the existence of low-order but dissimilar neighbor nodes in a path, messages from similar but high-order neighbor nodes are often weakened.

To tackle the challenges posed by heterophilic graphs, several advanced methods have been developed to enhance the message-passing mechanism Zheng et al. (2022); Luan et al. (2024). Approaches like blending high-order neighbors Zhu et al. (2020); Song et al. (2023); Wang & Derr (2021) and identifying potential neighbor nodes Pei et al. (2019); Suresh et al. (2021) aim to expand the effective neighborhood, but they may also amplify intermediate layers, introducing noise and over-reliance on irrelevant information. Other strategies focus on optimizing message aggregation, such as adaptive message aggregation Yan et al. (2022), layer-specific weight learning Chien et al. (2020), and diverse aggregation schemes Luan et al. (2022); Maurya et al. (2022); Du et al. (2022). Additionally,

¹<https://github.com/Anonymous-GloMP-GNN/GloMP-GNN>

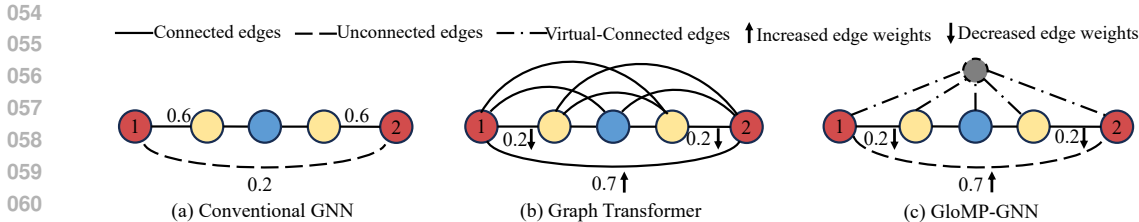


Figure 1: Illustration of different GNN methods in heterophilic graphs.

spectral methods differentiate between distinct-class neighbors using signed messages to capture high-frequency signals Yang et al. (2021); Bo et al. (2021). With continuous efforts, previous methods have alleviated the problem of the message-passing mechanism from different perspectives and achieved remarkable progress on heterophilic graphs.

However, few studies have fundamentally pointed out and solved the underlying problem, which is largely caused by the layer-by-layer localized nature of the current message-passing framework. Unlike these methods, we first theoretically and empirically analyze the localized layer-by-layer nature of the message-passing mechanism. Along this line, we propose to address the problem by introducing global insights into the message-passing mechanism. As illustrated in Figure 1, on heterophilic graphs, the message from similar but high-order neighbor nodes is often weakened by low-order dissimilar neighbor nodes in conventional GNN. Graph Transformer Shi et al. (2021) alleviates the issue by establishing global dependencies between nodes with fully-connected edges, but this will also greatly increase the extra quadratic computational complexity. Moreover, recent studies also reveal the over-globalizing problem Xing et al. (2024) in Graph Transformers with fully-connected edges. Unlike Graph Transformer, inspired by the concept of virtual node Gilmer et al. (2017b), we introduce global insights on heterophilic graphs by establishing virtual edges through a global virtual node, with only linear extra complexity.

To tackle the localized layer-by-layer nature of the message-passing mechanism, in this paper, we comprehensively introduce global insights into conventional message-passing mechanism and propose a novel Global Message-Passing Graph Neural Network (GloMP-GNN) for heterophilic graphs. To be concrete, the global insights of GloMP-GNN are reflected in two aspects. 1) During the message propagation phase, the global insight is introduced with a structure-based global propagation (SGP) strategy from the perspective of graph structure. By adding a global virtual node, messages between similar but high-order neighbor nodes can be effectively propagated with the bridge of virtual edges between the virtual node and graph nodes. Moreover, for redundant and noisy edges, a global edge adaption approach is included in SGP to adaptively aggregate messages by adjusting related edge weights; 2) During the feature updating phase, the global insight is introduced with a feature-augmented compensatory updating (FCU) method from the perspective of node feature. Through a multi-view feature updating mechanism, the node feature representation can be effectively augmented by compensating the weakened message from different views. The main contributions of our work are summarized as follows:

- We theoretically and empirically analyze the localized layer-by-layer nature of message-passing mechanisms. By comprehensively introducing global insights from both structure and feature perspectives, we propose GloMP-GNN with a global message-passing mechanism for heterophilic graphs.
- We propose a structure-based global propagation strategy by establishing virtual edges between the global virtual node and graph nodes. Moreover, a global edge adaption approach is included to aggregate messages with adaptive edge weight adjustment. In this way, messages between similar high-order neighbor nodes can be effectively propagated.
- We propose a feature-augmented compensatory updating method with multi-view feature updating mechanism. In this way, the node feature representation can be effectively augmented by compensating the weakened message from different views.
- Extensive experimental results on eight datasets demonstrate the superiority of our proposed GloMP-GNN. As broader impacts, GloMP-GNN consistently performs well across multiple layers and alleviates the over-smoothing issue.

2 PRELIMINARIES

2.1 BACKGROUND

Consider a graph $\mathcal{G} = (\mathcal{V}, \mathcal{E})$, where \mathcal{V} represents the set of nodes and \mathcal{E} denotes the set of edges. If nodes i and j are connected, then (i, j) is an edge in \mathcal{E} . The adjacency matrix of \mathcal{G} is represented by $\mathbf{A} \in \mathbb{R}^{N \times N}$, where $\mathbf{A}_{i,j} = 1$ if $(i, j) \in \mathcal{E}$ and $\mathbf{A}_{i,j} = 0$ otherwise. $N = |\mathcal{V}|$ indicates the number of nodes. The neighbor set of node i is $\mathcal{N}(i) = \{j : (i, j) \in \mathcal{E}\}$. Each node $i \in \mathcal{V}$ has an associated d dimensional feature vector $\mathbf{x}_i \in \mathbb{R}^d$ from the feature matrix $\mathbf{X} \in \mathbb{R}^{N \times d}$.

In the traditional GNN framework, the feature representation of each node is updated by aggregating information from its local neighbors. The process can be represented as:

$$\mathbf{m}_i^{(l)} = \text{AGG}^{(l)} \left(\left\{ \mathbf{x}_j^{(l-1)} : j \in \mathcal{N}(i) \right\} \right), \quad \mathbf{x}_i^{(l)} = \text{UPDATE}^{(l)} \left(\mathbf{x}_i^{(l-1)}, \mathbf{m}_i^{(l)} \right), \quad (1)$$

where $\mathbf{m}_i^{(l)}$ and $\mathbf{x}_i^{(l)}$ are the message vector and the feature representation of node i at layer l , respectively. The function $\text{AGG}^{(l)}$ and $\text{UPDATE}^{(l)}$ are the aggregation function and update function.

2.2 ANALYSIS ON MESSAGE-PASSING MECHANISM

The classic matrix representation for message-passing GNNs, like GCN and GAT Kipf & Welling (2016); Veličković et al. (2018), can be written as $\mathbf{X}^{(l)} = \sigma(\hat{\mathbf{A}}^{(l)} \mathbf{X}^{(l-1)} \mathbf{W}^{(l)})$. In GCN, $\hat{\mathbf{A}}^{(l)} = (\mathbf{D} + \mathbf{I})^{-1/2} (\mathbf{A} + \mathbf{D}) (\mathbf{D} + \mathbf{I})^{-1/2}$, where $\mathbf{D} = \text{diag}(\mathbf{A})$ is a diagonal matrix. In GAT, $\hat{\mathbf{A}}^{(l)} = \mathbf{A} \circ \mathbf{M}^{(l)}$, where \circ represents the element-wise multiplication, $\mathbf{M}^{(l)}$ represents the attention coefficient matrix at layer l . To simplify the mathematical exploration of model properties, following Eliasof et al. (2023); Azabou et al. (2023), the $\sigma(\cdot)$ function (*i.e.*, *ReLU*) is omitted in the following parts. Then, for traditional GNN models, $\mathbf{X}^{(l)} = \prod_{i=1}^l \hat{\mathbf{A}}^{(l-i+1)} \mathbf{X}^{(0)} \mathbf{W}^{(i)}$. Derivation details are listed in Appendix A.1.

In Graph Neural Networks (GNNs), the traditional qualitative descriptors of node relationships, such as similarity or strength, are insufficient for a detailed analysis of node interactions. We introduce influence intensity as a quantitative metric to overcome these limitations by measuring the exact degree of influence between nodes, accommodating both direct and indirect interactions. Specifically, we define the “Global Influence Intensity” and “Path Influence Intensity” as follows.

Definition 1 (Global Influence Intensity) In an l -layer GNN, the global influence intensity from node q to node p , denoted as $C_{p,q}$, is calculated by the matrix element $(\prod_{i=1}^l \hat{\mathbf{A}}^{(l-i+1)})_{p,q}$.

Definition 2 (Path Influence Intensity) The influence intensity of node q on node p along a specific path $P = (p, i_1, i_2, \dots, i_{k-1}, q)$ is denoted as $C_{p,q}^P$, which is computed based on the weights along path P .

Obviously, the Global Influence Intensity from node q to node p can be calculated by adding all the Path Influence Intensity of node q on node p . Under the definition of influence intensity, it’s obvious that for a specific path $P = (i, j)$, $C_{i,j}^P = \hat{\mathbf{A}}_{i,j}$, where edge weight and influence intensity between node i and j are numerically identical.

Considering that there may be multiple paths between two nodes in a graph, the two nodes may be different order neighbors on different paths. In order to unify the description, we define the neighbor orders of nodes as follows.

Definition 3 (k-order Neighbors) The k -order neighbors of a node p in a graph encompass all neighbors that are at a minimum hop of k from the node p , denoted as $\mathcal{N}^{(k)}(p)$.

Along with the previous introduction, we intend to investigate the propagation of the influence intensity in the message-passing mechanism. Taking the widely adopted GCN and GAT as illustrative examples, we perform an in-depth analysis of 10-layer GNNs.

From Figure 2(a), we observe a consistent trend for both GCN and GAT. As the order of neighbors increases, the averaged global influence intensity begins to decrease. From Figure 2(b), we can

162
163
164
165
166
167
168
169
170
171
172
173
174
175
176
177
178
179
180
181
182
183
184
185
186
187
188
189
190
191
192
193
194
195
196
197
198
199
200
201
202
203
204
205
206
207
208
209
210
211
212
213
214
215

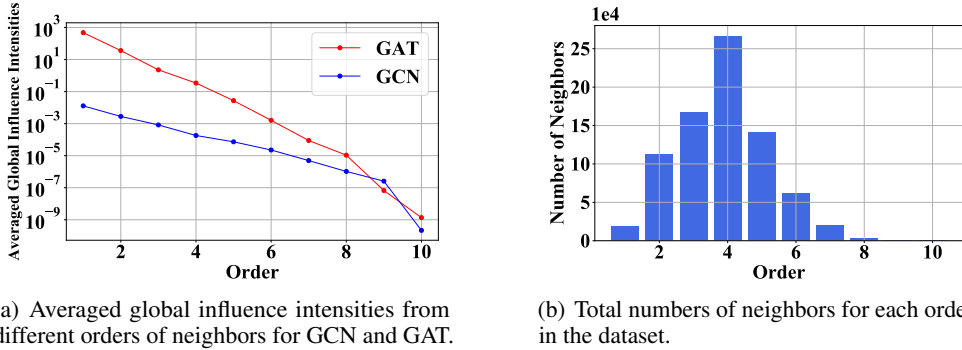


Figure 2: Propagation of node influence intensity for GCN and GAT (10 layers) in the filtered Chameleon dataset Platonov et al. (2023).

observe that in a heterophilic graph, the number of nodes with high-order neighbors (for example, greater than 3) actually accounts for a very large proportion. However, the trend in Figure 2(a) implies that the influence of these high-order neighbors on the central node is extremely low. This tendency may be detrimental to capturing the broader structure in heterophilic graphs, where insights from higher-order neighbors are essential Zhu et al. (2020); Song et al. (2023).

The above illustration uses empirical analysis to show the global influence intensity between nodes in a graph under the layer-by-layer nature. Building upon these empirical findings, we now proceed with a theoretical examination to further demonstrate how the path influence intensity between nodes may be diminished by the inherent nature of the layer-by-layer message-passing mechanism.

Theorem 1 *In traditional GNN models, for any given node i_0 and its k -order neighbor i_k along any path $\mathcal{P} = (i_0, i_1, i_2, i_3, \dots, i_k)$ within a heterophilic graph $\mathcal{G} = (\mathcal{V}, \mathcal{E})$, the path influence intensity of i_k to i_0 (i.e., $C_{i_0, i_k}^{\mathcal{P}}$) approaches zero as k tends towards infinity, i.e.,*

$$\lim_{k \rightarrow \infty} C_{i_0, i_k}^{\mathcal{P}} = 0.$$

The proof of the theorem is deferred to Appendix A.1. This theorem highlights the intrinsic limitation of the layer-by-layer nature of the message-passing mechanism, particularly in heterophilic graphs. In such graphs, nodes that are close yet dissimilar might receive lower influence weights, potentially weakening the contribution of distant but similar nodes in the same path. Although recent models like JKNet Xu et al. (2018), GPRGNN Chien et al. (2020) and GCNII Chen et al. (2020) have introduced residual connections to preserve self-information and jumping links or learning weights separately for each layer, the influence intensities of distant nodes can hardly benefit from this. Since an increase in the weight of a distant layer can affect the weights of intermediate layers, this may introduce noise and an overreliance on intermediate layers that may contain irrelevant or even harmful data. As a result, the influence intensities from high-order neighbors are very small, presenting a challenge in capturing valuable information from distant nodes for heterophilic graphs.

3 GLOMP-GNN

In this section, we will present our proposed GloMP-GNN with a global message-passing mechanism for heterophilic graphs in detail. Overall, GloMP-GNN comprehensively introduces global insights from two aspects. (1) From the perspective of graph structure, a structure-based global propagation strategy is designed in the message propagation phase. (2) From the perspective of node feature, a feature-augmented compensatory updating method is developed in the feature updating phase. The technical details of GloMP-GNN are presented as follows.

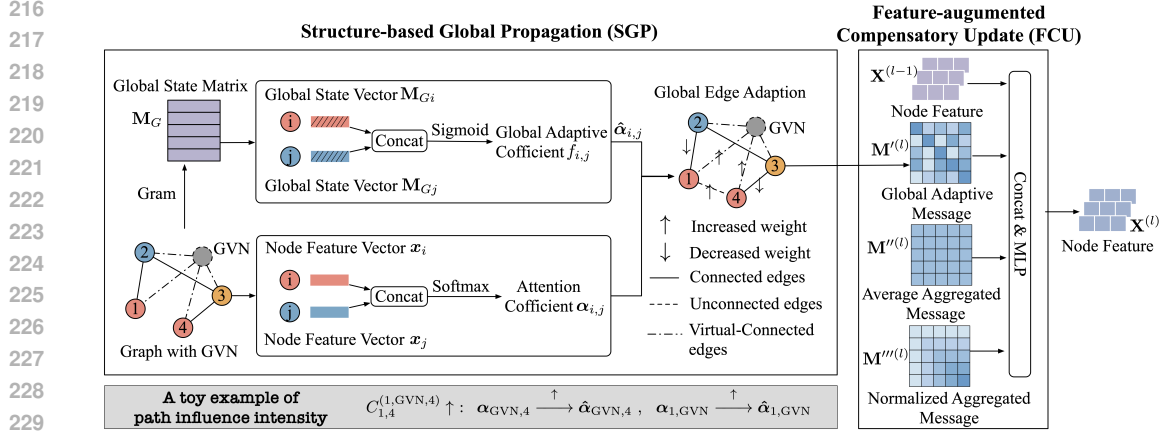


Figure 3: The framework of GloMP-GNN, which consists of a Structure-based Global Propagation module and a Feature-augmented Compensatory Update module. A toy example of path influence intensity illustrates that, with GVN and Global Edge Adaption in SGP, the path influence intensity from node 4 to node 1 can be increased.

3.1 STRUCTURE-BASED GLOBAL PROPAGATION

Inspired by the concept of virtual node Gilmer et al. (2017b); Cai et al. (2023), we add a Global Virtual Node (GVN) to connect every node in the graph. Then, virtual-connected edges between the GVN and graph nodes can be established. In this way, messages between similar but high-order neighbor nodes can be effectively propagated with the bridge of virtual edges. Therefore, the following theorem can be formulated:

Theorem 2 *In graph \mathcal{G} , if a global virtual node is added to connect every node on the graph, then for any node on the graph, its maximum neighbor order is 2.*

Based on Theorem 2, messages can be effectively and efficiently propagated between similar but high-order neighbor nodes in heterophilic graphs.

For technical details, the feature representation of GVN (*i.e.*, \mathbf{x}_{GVN}) is initialized as:

$$x_{\text{GVN},i} = \max_{u \in \mathcal{V}} x_{u,i}, \quad (2)$$

where $x_{\text{GVN},i}$ is the feature representation of the GVN for the i^{th} dimension. \mathcal{V} represents all nodes in the graph, $x_{u,i}$ is the feature representation of node u for the i^{th} dimension.

Despite the effectiveness of the virtual node in information propagation, it may also introduce some redundant and noisy edges, which interfere with the learning process and degrade model performance Hu et al. (2020; 2021).

Along this line, we further design a Global Edge Adaption (GEA) approach to adaptively adjust the weights of those edges. Specifically, we firstly leverage the multi-head attention mechanism to learn different weights of neighbors, which can be calculated as follows:

$$\alpha_{ij} = \text{Softmax}(\text{LeakyReLU}(\mathbf{a}^T[\mathbf{W}_A \mathbf{x}_i \parallel \mathbf{W}_A \mathbf{x}_j])). \quad (3)$$

Here, $[\cdot \parallel \cdot]$ denotes concatenation, \mathbf{a} is a learnable weight parameter vector, and \mathbf{W}_A is a learnable weight parameter matrix.

Next, we introduce a global state matrix \mathbf{M}_G , which leverages the Gram matrix Sreeram & Agathoklis (1994) to encapsulate the relationships of all nodes based on their initial feature representations. Here, the Gram matrix is defined as $\text{Gram} = \mathbf{X}^{(0)} \mathbf{X}^{(0)T}$, where $\mathbf{X}^{(0)}$ represents the initial feature matrix of the nodes. Moreover, we incorporate a noise matrix (*i.e.*, $\mathbf{M}_{\text{noise}}$) into \mathbf{M}_G , which serves as a proxy for potential uncertainties and variances inherent in real-world datasets. Thus, the generalization

ability and robustness of our proposed method could be improved. The formulation is written as follows:

$$\mathbf{M}_G = Gram \cdot \mathbf{W}_G + \epsilon \cdot \mathbf{M}_{\text{noise}}, \quad (4)$$

where \mathbf{W}_G and ϵ are trainable weight parameters. $\mathbf{M}_{\text{noise}} \sim \mathcal{N}(0, 1)$ is sampled from the standard normal distribution.

Based on the global state matrix \mathbf{M}_G , we calculated the global adaptive coefficient $f_{i,j}$ for connected nodes i and j based on their global state representations as follows:

$$f_{i,j} = \sigma([\mathbf{M}_{G_i} \parallel \mathbf{M}_{G_j}] \cdot \mathbf{W}_f + \mathbf{b}_f), \quad (5)$$

where $[\mathbf{M}_{G_i} \parallel \mathbf{M}_{G_j}]$ denotes the concatenation of the global state vectors of nodes i and j , \mathbf{W}_f and \mathbf{b}_f are learnable weight matrix and bias term. $\sigma(\cdot)$ is the sigmoid activation function that ensures the global adaptive coefficients are constrained in the range $[0, 1]$.

Then, a new global multi-head attention coefficient $\hat{\alpha}_{i,j}$ can be obtained by integrating the global adaptive coefficient $f_{i,j}$ with the original multi-head attention coefficient $\alpha_{i,j}$. This process is formulated as follows:

$$\hat{\alpha}_{i,j} = \text{Softmax}(\beta(f_{i,j} \cdot \alpha_{i,j}) + (1 - \beta)\alpha_{i,j}), \quad (6)$$

where $\beta \in [0, 1]$ is a trainable parameter that balances the influence of the adaptively adjusted attention coefficient and original attention coefficient. This formulation can enhance our model ability to capture global dependencies between nodes.

Finally, based on the global attention coefficients $\hat{\alpha}_{i,j}$, the message is propagated and aggregated.

$$\mathbf{m}_i^{(l)} = \sigma \left(\sum_{j \in \mathcal{N}(i)} \hat{\alpha}_{i,j}^{(l-1)} \mathbf{W}^{(l-1)} \mathbf{x}_j^{(l-1)} \right), \quad (7)$$

where $\mathbf{m}_i^{(l)}$ is the aggregated message at l^{th} layer for node i after aggregating information from its neighbors at $(l-1)^{\text{th}}$ layer, $\mathbf{W}^{(l-1)}$ is a learnable weight matrix. Additionally, $\mathbf{M}^{(l)} = \{\mathbf{m}_i^{(l)}\}_{i=0}^N$ represent the global adaptive message matrix at l^{th} layer.

3.2 FEATURE-AUGMENTED COMPENSATORY UPDATE

As stated before, in heterophilic graphs, messages from similar but high-order neighbor nodes are often weakened due to the local nature of the layer-by-layer message-passing mechanism. To this end, during the message propagation phase, as presented before, we design the SGP strategy to introduce global insight from the perspective of graph structure. In addition, during the feature updating phase, we also develop a feature-augmented compensatory updating method to introduce global insight from the perspective of node feature. Specifically, we comprehensively utilize three different message aggregation mechanisms for multi-view feature updating. In this way, messages weakened in a single view can be mutually compensated by messages from other views.

The first is the aggregation mechanism from GEA, which provides an attention-based global adaptive view. The second is the average aggregation mechanism, which provides an edge-balanced view. It is formulated as follows:

$$\mathbf{m}_i''^{(l)} = \sigma \left(\mathbf{W}''^{(l-1)} \frac{\sum_{j \in \mathcal{N}(i)} \mathbf{x}_j^{(l-1)}}{|\mathcal{N}(i)|} \right). \quad (8)$$

Thus, the average aggregated message matrix at l^{th} layer can be written as $\mathbf{M}''^{(l)} = \{\mathbf{m}_i''^{(l)}\}_{i=0}^N$.

The third is the normalized aggregation mechanism, which provides a node degree-based view. It can be represented as follows:

$$\mathbf{m}_i'''^{(l)} = \sigma \left(\mathbf{W}'''^{(l-1)} \sum_{j \in \mathcal{N}(i)} \frac{\mathbf{x}_j^{(l-1)}}{\sqrt{\text{degree}(i) \times \text{degree}(j)}} \right). \quad (9)$$

Then, the normalized aggregated message matrix at l^{th} layer can be written as $\mathbf{M}'''^{(l)} = \{\mathbf{m}_i'''^{(l)}\}_{i=0}^N$.
 By bringing multi-view messages all together, the representation of node i will be updated with a fusion of its own features and aggregated messages using a multi-layer perceptron (MLP) with two hidden layers and Gelu activation. It is represented as follows:

$$\mathbf{x}_i^{(l)} = \text{MLP}([\mathbf{x}_i^{(l-1)} \parallel \mathbf{m}_i''^{(l)} \parallel \mathbf{m}_i'''^{(l)}]), \quad (10)$$

where $[\cdot \parallel \cdot]$ denotes the concatenation operation.

In this way, our proposed FCU method comprehensively utilizes messages in different views and augments the node feature updating process. Thus, FCU is capable of overcoming the local nature of current message-passing mechanisms from the perspective of node features.

4 EXPERIMENTS

4.1 DATASETS

To investigate the performance of our model across various datasets, we conduct experiments on five heterophilic datasets (Actor Pei et al. (2019), Roman-empire Lhoest et al. (2021); Platonov et al. (2023), Amazon-ratings Leskovec & Krevl (2014); Platonov et al. (2023), Minesweeper Platonov et al. (2023), and Tolokers Platonov et al. (2023)), and three commonly used homophilic datasets (Cora, CiteSeer, PubMed Sen et al. (2008)). For a more comprehensive measurement of dataset heterophily, we use two metrics: h_{edge} Pei et al. (2019) and label informativeness (LI) Platonov et al. (2024). More descriptions of these datasets and heterophily metrics are listed in the Appendix A.2.

4.2 BASELINES

To verify the effectiveness of the proposed GloMP-GNN on the node classification task, 18 methods are employed as baselines, which can be divided into five groups: (1) deep learning method ResNet He et al. (2016); (2) classic GNN models, such as GCN Kipf & Welling (2016), GraphSage Hamilton et al. (2017), GAT Veličković et al. (2018) and GATv2 Brody et al. (2022); (3) selective information propagation method, such as H₂GCN Zhu et al. (2020), GBK-GNN Du et al. (2022), GCNII Chen et al. (2020), FSGNN Maurya et al. (2022), and OrderedGNN Song et al. (2023); (4) graph signal-based methods, such as GPR-GNN Chien et al. (2020), FAGCN Bo et al. (2021), JacobiConv Wang & Zhang (2022) and ALT-APPNP Xu et al. (2023); (5) global information-based method, such as Graph Transformer (GT) Shi et al. (2021), GraphGPS Rampásek et al. (2022), GloGNN++ Li et al. (2022) LRGNN Liang et al. (2024). More descriptions and analysis of these baselines are listed in the Appendix A.2.

4.3 EXPERIMENTAL SETUP

All experiments are implemented with PyTorch Paszke et al. (2019) and DGL Wang et al. (2019) on a Linux server equipped with six 2.30GHz Intel (R) Xeon (R) Gold 5218 CPUs and an NVIDIA Tesla V100-SXM2-32GB GPU. All models are trained with the Adam optimizer Kingma & Ba (2015). For GloMP-GNN, we explore a range of hyperparameters: learning rates are chosen from $\{1e-2, 1e-3, 1e-4, 3e-4, 1e-5, 3e-5\}$, hidden dimensions are taken from $\{64, 128, 256, 512\}$, the number of attention heads is set to 4 or 8, and the number of hidden layers varies from 1 to 10. For baselines, the experimental parameter settings are based on the hyperparameters provided in original papers, datasets, and our computational resources. All the models are tuned to be optimal to ensure fair comparisons. Models are trained for 1,000 epochs on ten 50%/25%/25% train/validation/test splits in heterophilic datasets and ten 60%/20%/20% train/validation/test splits in homophilic datasets. We select models based on the best validation set performance. Following Platonov et al. (2023); Müller et al. (2024), for a fair comparison, we also adopt Accuracy as evaluation metrics on Actor, Roman, Amazon, Cora, Citeseer and Pubmed datasets, and adopt AUC as metrics on Minesweeper and Tolokers datasets.

Table 1: Performance of GloMP-GNN and other popular GNN models on both heterophily and homophily graph datasets.

Model	Actor	Roman	Amazon	Minesweeper	Tolokers	Cora	Citeseer	Pubmed
ResNet	33.47±0.75	65.88±0.38	45.90±0.52	50.89±1.39	72.95±1.06	74.95±2.09	72.90±1.70	86.78±0.38
GCN	34.96±1.10	73.69±0.74	48.70±0.63	89.75±0.52	83.64±0.67	86.60±0.95	75.88±1.52	88.18±0.50
GraphSage	35.68±0.72	85.74±0.67	53.63±0.39	93.51±0.57	82.43±0.44	86.66±1.42	76.29±1.88	88.83±0.50
GAT	34.82±1.17	80.87±0.30	49.09±0.63	92.01±0.68	83.70±0.47	86.80±1.02	75.93±1.38	87.82±0.43
GATv2	35.66±0.70	85.69±0.57	49.71±0.68	91.53±0.66	82.93±0.62	86.73±1.15	75.86±1.73	87.81±0.52
H2GCN	35.09±1.00	60.11±0.52	36.47±0.23	89.71±0.31	73.35±0.01	87.12±0.81	77.04±1.15	88.53±0.42
GBK-GNN	34.38±0.67	74.57±0.47	45.98±0.71	90.85±0.58	81.01±0.67	86.74±0.74	76.15±2.02	88.79±0.53
GCNII	34.88±0.85	79.33±0.56	49.70±0.68	89.64±1.18	84.89±0.54	86.12±0.88	76.24±1.83	88.80±0.43
FSGNN	35.21±0.66	79.92±0.56	52.74±0.83	90.08±0.70	82.76±0.61	85.49±1.15	75.65±1.42	89.31±0.37
OrderedGNN	36.01±1.13	81.92±0.79	52.35±0.55	90.13±1.77	81.85±0.87	86.96±1.44	75.48±1.73	89.07±0.52
GPR-GNN	34.70±0.86	64.85±0.27	44.88±0.34	86.24±0.61	72.94±0.97	87.63±1.59	77.15±1.67	88.58±0.48
FAGCN	34.95±1.36	65.22±0.56	44.12±0.30	88.17±0.73	77.75±1.05	87.89±0.85	76.35±1.12	89.32±0.28
JacobiConv	35.54±0.85	71.14±0.42	43.55±0.48	89.66±0.40	68.66±0.65	86.76±0.98	76.42±1.36	89.02±0.39
ALT-APPNP	32.41±1.27	69.13±0.43	43.81±0.37	80.19±0.26	78.60±0.62	85.01±0.86	73.54±0.60	89.06±0.48
GT	33.86±1.04	86.51±0.73	51.17±0.66	91.85±0.76	83.23±0.64	86.76±1.30	75.80±1.53	87.17±0.58
GraphGPS	36.53±0.68	87.04±0.58	51.03±0.60	93.85±0.41	84.81±0.86	86.56±1.01	76.02±1.17	88.94±0.57
GloGNN++	35.42±0.76	59.63±0.69	36.89±0.14	51.08±1.23	73.39±1.17	88.33±1.09	77.22±1.78	89.24±0.39
LRGNN	36.86±0.86	62.29±1.33	36.79±0.49	80.00±0.00	78.51±0.38	88.26±1.02	75.19±1.51	89.26±0.62
GloMP-GNN	37.04±0.80	90.21±0.62	53.72±0.41	96.32±0.42	85.11±0.64	87.53±1.32	76.87±1.12	89.72±0.37

Table 2: Ablation Performance (%) of GloMP-GNN on different datasets.

Model	Actor	Roman	Amazon	Minesweeper	Tolokers	Cora	Citeseer	Pubmed
(1) w/o GVN	36.12	89.51	52.71	95.05	84.51	86.57	75.84	88.80
(2) w/o GEA	36.80	89.47	52.82	95.11	84.14	86.46	75.21	89.12
(3) w/o \mathbf{m}'	36.87	86.82	52.72	94.62	84.06	86.31	75.72	89.48
(4) w/o \mathbf{m}''	36.64	88.53	53.03	95.40	83.74	85.71	75.47	88.95
(5) w/o \mathbf{m}'''	36.43	88.33	52.12	95.67	83.60	86.92	75.32	88.84
(6) GloMP-GNN	37.04	90.21	53.72	96.32	85.11	87.53	76.87	89.72

4.4 PERFORMANCES ON DIFFERENT DATASETS

We evaluate different methods on the aforementioned 8 datasets, following the same data splits as Pei et al. (2019); Platonov et al. (2023). As shown in Table 1, we report the average performance with the standard deviation on test sets over 10 data splits.

Compared with various state-of-the-art models across homophilic datasets and heterophilic datasets, GloMP-GNN is the most reliable and effective model across a wide range of datasets, demonstrating its superiority and robustness. Furthermore, it is observed that traditional GNN methods tend to outperform methods designed for heterophily on many datasets. This aligns with the issues identified in Platonov et al. (2023), indicating that current heterophilic graph models still have significant room for improvement. In Tolokers, edges are relatively dense, and the excellent performance of our model demonstrates the ability of the Global Edge Adaption (GEA) module to adjust edge weights adaptively. Conversely, in Roman-empire, which has sparser edges, the models that perform well are those that incorporate global context by allowing nodes to attend to information from distant parts of the graph, rather than just their immediate neighbors, such as GT and our GloMP-GNN. This highlights the exceptional capability of our GloMP-GNN in capturing a global perspective and effectively learning information from distant nodes. These observations from the two datasets demonstrate the effectiveness of GloMP-GNN in both sparse and dense datasets. In addition, we also perform time analysis to show the efficiency of GloMP-GNN in Appendix A.4.

4.5 ABLATION STUDY

To investigate the effectiveness of different components in GloMP-GNN, we further conduct ablation studies on different variants of our proposed GloMP-GNN. In the message propagation phase, as shown in Table 2 (1)-(2), when removing GVN and GEA separately, the performance of GloMP-GNN decreased with different degrees, which demonstrates both GVN and GEA are critical for introducing global properties in the message-passing mechanism and improve model performance.

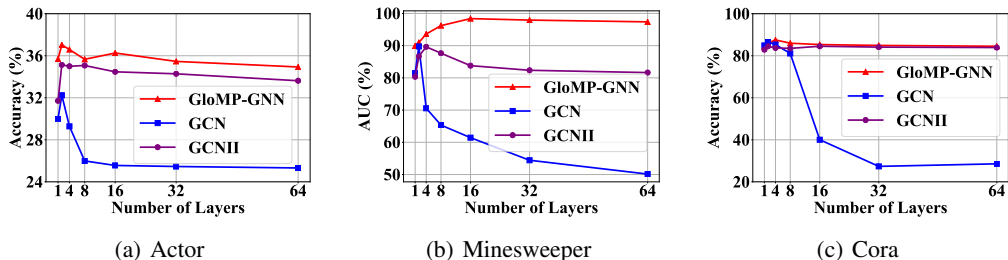


Figure 4: Node classification performances for over-smoothing problems with various depths.

In the feature updating phase, GloMP-GNN updates node features by comprehensively taking into account messages (*i.e.*, \mathbf{m}' , \mathbf{m}'' and \mathbf{m}''') from different views. As shown in Table 2 (3)-(5), the performance of GloMP-GNN decreases with varying degrees when removing any message, which again illustrates the importance and benefits of our proposed multi-view feature updating mechanism.

4.6 OVER-SMOOTHING PROBLEM

To validate the ability of GloMP-GNN to mitigate over-smoothing, we compare its performance with GCN and GCNII on three datasets: Actor, Minesweeper, and Cora. In particular, GCNII is an approach specially designed to alleviate the over-smoothing issue. As shown in Figure 4, on the heterophilic Actor dataset, GloMP-GNN shows consistent performance across all layers, whereas GCN fluctuates, and although GCNII demonstrates moderate stability, its performance is not as strong as GloMP-GNN. On the heterophilic Minesweeper dataset, GloMP-GNN improves with increasing depth, while both GCN and GCNII decline, suggesting that GloMP-GNN effectively adapts to deeper networks. On the homophilic Cora dataset, GloMP-GNN peaks at the 4th layer and maintains high accuracy with only a slight decline at 64 layers, while GCN exhibits significant drops in performance as depth increases. In summary, GloMP-GNN consistently alleviates over-smoothing, demonstrating its effectiveness across various graph structures and evaluation metrics. In addition, we also quantify the ability of GloMP-GNN to mitigate over-smoothing through Dirichlet Energy Karhadkar et al. (2023), which is shown in Appendix A.5.

4.7 CASE STUDY AND VISUALIZATION

Visualization of Node Features. On heterophilic graphs, node features learned in multi-layer GNNs are prone to over-smoothing. To investigate the ability of GloMP-GNN to solve the over-smoothing problem, we further conduct experiments on a heterophilic dataset (*i.e.*, Roman-empire). Specifically, we used t-SNE Van der Maaten & Hinton (2008) to visualize node representations learned on the 64-layer GCN and GloMP-GNN. The results are shown in the Figure 5. It is obvious that compared to GCN, node representations learned by GloMP-GNN are more discriminative. That is, intra-class node representations are close together, while inter-class node representations are far apart. The visualization results illustrate the potential ability of GloMP-GNN to alleviate the over-smoothing problem in multi-layer graph neural networks on heterophilic graphs.

Case Study on Global Edge Adaption. We also conduct a case study on the edge weight adjustment process by the Global Edge Adaption (GEA). For the convenience of observation and display, we have set the number of attention heads to 1 here. Taking the Roman-empire dataset as an example, as illustrated in Figure 6, each circle represents a node, with the corresponding ID below it. In the figure, the edge coefficient formed by nodes with node 1 and 2 is been reduced to a value close to 0, even though the original attention coefficient from node 2 to node 1 is relatively high at 0.6469, likely due to the similarity between their features, as computed in Equation 3. To analyze the reason, we investigated the 1-order and 2-order neighbors of node 2 and found that none of these neighbors belong to the same label as node 1. Therefore, the contribution of node 2 to node 1 is minimal. This demonstrates that GEA is capable of incorporating global information, effectively removing redundant and detrimental edges, thereby enhancing the accuracy of model learning.

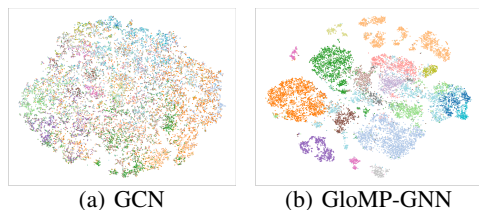


Figure 5: Comparison of GCN and GloMP-GNN visualizations obtained from 64 layers of feature representations in two-dimensional space on Roman-empire dataset.

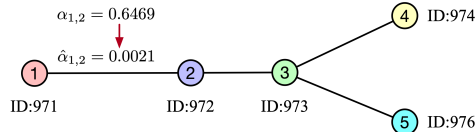


Figure 6: Example of edge weight adjustment by GEA within the Roman Empire dataset, where different colors represent different node labels.

5 RELATED WORK

In heterophilic graph neural networks, various strategies have been proposed to enhance effectiveness Zheng et al. (2022); Zhu et al. (2023); Khoshraftar & An (2024). A central approach is ego- and neighbor-embedding separation, effectively employed by models such as H₂GCN Zhu et al. (2020) and FSGNN Maurya et al. (2022). Building on this, H₂GCN and TDGNN Wang & Derr (2021) aggregate higher-order neighborhood information across layers. Other methods focus on aggregation strategies, like OrderedGNN Song et al. (2023), which aligns the hierarchy of rooted trees with neuron order, adaptive channel mixing in ACM-GNN Luan et al. (2022), and gated kernels in GBK-GNN Du et al. (2022). While these methods enhance the internal structures of GNNs, models like Geom-GCN Pei et al. (2019) and WRGNN Suresh et al. (2021) refine the message-passing mechanisms for heterophilic graphs Qiu et al. (2024); Pan & Kang (2023), though they often involve complex, dataset-specific designs, limiting their generalizability. Additionally, spectral methods like GPR-GNN Chien et al. (2020), BernNet He et al. (2021), JocabiConv Wang & Zhang (2022), ALT Xu et al. (2023), and FAGCN Bo et al. (2021) use signed messages to capture high-frequency signals. However, these methods may suffer from the “negative times negative equals positive” effect, which is problematic for multi-class heterophilic graphs Liang et al. (2024). More recently, global information has been incorporated into models, including message-passing-based methods Li et al. (2022); Liang et al. (2024), and Graph Transformer-based methods Shi et al. (2021); Rampášek et al. (2022); Chen et al. (2023); Fu et al. (2024). However, these approaches incorporate global context through external mechanisms, such as global coefficient matrices or self-attention, without addressing the inherent limitations of the layer-by-layer structure in the message-passing mechanism.

Recent analyses have uncovered issues with several widely-used heterophilic graph datasets Platonov et al. (2023). For instance, datasets like *Squirrel* and *Chameleon* suffer from data leakage due to duplicate nodes, while smaller datasets such as *Cornell*, *Texas*, and *Wisconsin* face class imbalance and limited size (fewer than 1K nodes). Additionally, evaluations of heterophilic GNN models on new, larger datasets (10K-50K nodes) revealed that these advanced models often underperform, even lagging behind traditional GNNs like GCN Kipf & Welling (2016), GAT Veličković et al. (2018), and GraphSAGE Hamilton et al. (2017). Thus, there is a need for more profound analysis to understand the underlying causes and to develop solutions that are more robust and adaptable for real-world graph scenarios.

6 CONCLUSION

In this paper, we first conducted both theoretical and empirical analysis of the localized layer-by-layer nature of the message-passing mechanism. Then, we introduced a Global Message-passing Graph Neural Network (GloMP-GNN) for heterophilic graphs. By innovatively integrating a structure-based global propagation and a feature-augmented compensatory update module into the message-passing framework, GloMP-GNN effectively addresses the issue where messages from high-order but similar neighbor nodes are often weakened during propagation. We hope that our work will inspire further research in this direction. In future work, we plan to extend GloMP-GNN to other graph mining tasks, such as graph classification and downstream tasks like anomaly detection, as well as explore its potential in handling various types of graph data, such as heterogeneous graphs and hypergraphs.

REFERENCES

- 540
541
542 Mehdi Azabou, Venkataramana Ganesh, Shantanu Thakoor, Chi-Heng Lin, Lakshmi Sathidevi, Ran
543 Liu, Michal Valko, Petar Veličković, and Eva L Dyer. Half-hop: A graph upsampling approach for
544 slowing down message passing. In *International Conference on Machine Learning*, pp. 1341–1360.
545 PMLR, 2023.
- 546 Deyu Bo, Xiao Wang, Chuan Shi, and Huawei Shen. Beyond low-frequency information in graph con-
547 volutional networks. In *Proceedings of the AAAI Conference on Artificial Intelligence*, volume 35,
548 pp. 3950–3957, 2021.
- 549 Shaked Brody, Uri Alon, and Eran Yahav. How attentive are graph attention networks? In *International
550 Conference on Learning Representations*, 2022.
- 551
552 Chen Cai, Truong Son Hy, Rose Yu, and Yusu Wang. On the connection between mpnn and graph
553 transformer. In *International Conference on Machine Learning*. PMLR, 2023.
- 554
555 Jinsong Chen, Kaiyuan Gao, Gaichao Li, and Kun He. NAGphormer: A tokenized graph transformer
556 for node classification in large graphs. In *The Eleventh International Conference on Learning
557 Representations*, 2023.
- 558
559 Ming Chen, Zhewei Wei, Zengfeng Huang, Bolin Ding, and Yaliang Li. Simple and deep graph
560 convolutional networks. In *International conference on machine learning*, pp. 1725–1735. PMLR,
561 2020.
- 562
563 Eli Chien, Jianhao Peng, Pan Li, and Olgica Milenkovic. Adaptive universal generalized pagerank
564 graph neural network. In *International Conference on Learning Representations*, 2020.
- 565
566 Lun Du, Xiaozhou Shi, Qiang Fu, Xiaojun Ma, Hengyu Liu, Shi Han, and Dongmei Zhang. Gbk-
567 gnn: Gated bi-kernel graph neural networks for modeling both homophily and heterophily. In
568 *Proceedings of the ACM Web Conference 2022*, pp. 1550–1558, 2022.
- 569
570 Moshe Eliasof, Lars Ruthotto, and Eran Treister. Improving graph neural networks with learnable
571 propagation operators. In *International Conference on Machine Learning*, pp. 9224–9245. PMLR,
572 2023.
- 573
574 Dongqi Fu, Zhigang Hua, Yan Xie, Jin Fang, Si Zhang, Kaan Sancak, Hao Wu, Andrey Malevich, Jin-
575 grui He, and Bo Long. VCR-graphormer: A mini-batch graph transformer via virtual connections.
576 In *The Twelfth International Conference on Learning Representations*, 2024.
- 577
578 Justin Gilmer, Samuel S Schoenholz, Patrick F Riley, Oriol Vinyals, and George E Dahl. Neural
579 message passing for quantum chemistry. In *International conference on machine learning*, pp.
580 1263–1272. PMLR, 2017a.
- 581
582 Justin Gilmer, Samuel S Schoenholz, Patrick F Riley, Oriol Vinyals, and George E Dahl. Neural
583 message passing for quantum chemistry. In *International conference on machine learning*, pp.
584 1263–1272. PMLR, 2017b.
- 585
586 Will Hamilton, Zhitao Ying, and Jure Leskovec. Inductive representation learning on large graphs. In
587 *Advances in neural information processing systems*, volume 30, 2017.
- 588
589 Kaiming He, Xiangyu Zhang, Shaoqing Ren, and Jian Sun. Deep residual learning for image
590 recognition. In *Proceedings of the IEEE conference on computer vision and pattern recognition*,
591 pp. 770–778, 2016.
- 592
593 Mingguo He, Zhewei Wei, Hongteng Xu, et al. Bernnet: Learning arbitrary graph spectral filters via
bernstein approximation. *Advances in Neural Information Processing Systems*, 34:14239–14251,
2021.
- Wenhua Hu, Matthias Fey, Marinka Zitnik, Yuxiao Dong, Hongyu Ren, Bowen Liu, Michele Catasta,
and Jure Leskovec. Open graph benchmark: Datasets for machine learning on graphs. *Advances in
neural information processing systems*, 33:22118–22133, 2020.

- 594 Weihua Hu, Matthias Fey, Hongyu Ren, Maho Nakata, Yuxiao Dong, and Jure Leskovec. Ogb-lsc: A
595 large-scale challenge for machine learning on graphs. *NeurIPS*, 34, 2021.
- 596
- 597 Haitao Huang, Hu Tian, Xiaolong Zheng, Xingwei Zhang, Daniel Dajun Zeng, and Fei-Yue Wang.
598 Cggn: A compatibility-aware graph neural network for social media bot detection. *IEEE Transac-*
599 *tions on Computational Social Systems*, 2024.
- 600 Kedar Karhadkar, Pradeep Kr. Banerjee, and Guido Montufar. FoSR: First-order spectral rewiring
601 for addressing oversquashing in GNNs. In *The Eleventh International Conference on Learning*
602 *Representations*, 2023.
- 603
- 604 Shima Khoshraftar and Aijun An. A survey on graph representation learning methods. *ACM*
605 *Transactions on Intelligent Systems and Technology*, 15(1):1–55, 2024.
- 606 D Kingma and J Ba. Adam: A method for stochastic optimization. *Proceedings of the 3rd interna-*
607 *tional conference for learning representations*, 500, 2015.
- 608
- 609 Thomas N Kipf and Max Welling. Semi-supervised classification with graph convolutional networks.
610 In *International Conference on Learning Representations*, 2016.
- 611 Jure Leskovec and Andrej Krevl. Snap datasets: Stanford large network dataset collection, 2014.
- 612
- 613 Quentin Lhoest, Albert Villanova del Moral, Yacine Jernite, Abhishek Thakur, Patrick von Platen,
614 Suraj Patil, Julien Chaumond, Mariama Drame, Julien Plu, Lewis Tunstall, et al. Datasets: A
615 community library for natural language processing. In *Proceedings of the 2021 Conference on*
616 *Empirical Methods in Natural Language Processing: System Demonstrations*, pp. 175–184, 2021.
- 617 Xiang Li, Renyu Zhu, Yao Cheng, Caihua Shan, Siqiang Luo, Dongsheng Li, and Weining Qian.
618 Finding global homophily in graph neural networks when meeting heterophily. In *International*
619 *Conference on Machine Learning*, pp. 13242–13256. PMLR, 2022.
- 620
- 621 Langzhang Liang, Xiangjing Hu, Zenglin Xu, Zixing Song, and Irwin King. Predicting global label
622 relationship matrix for graph neural networks under heterophily. *Advances in Neural Information*
623 *Processing Systems*, 36, 2024.
- 624 Tianyu Liu, Yuge Wang, Rex Ying, and Hongyu Zhao. Muse-gnn: learning unified gene representation
625 from multimodal biological graph data. *Advances in neural information processing systems*, 36,
626 2024.
- 627 Sitao Luan, Chenqing Hua, Qincheng Lu, Jiaqi Zhu, Mingde Zhao, Shuyuan Zhang, Xiao-Wen
628 Chang, and Doina Precup. Revisiting heterophily for graph neural networks. *Advances in neural*
629 *information processing systems*, 35:1362–1375, 2022.
- 630
- 631 Sitao Luan, Chenqing Hua, Qincheng Lu, Liheng Ma, Lirong Wu, Xinyu Wang, Minkai Xu, Xiao-Wen
632 Chang, Doina Precup, Rex Ying, et al. The heterophilic graph learning handbook: Benchmarks,
633 models, theoretical analysis, applications and challenges. *arXiv preprint arXiv:2407.09618*, 2024.
- 634 Sunil Kumar Maurya, Xin Liu, and Tsuyoshi Murata. Simplifying approach to node classification in
635 graph neural networks. *Journal of Computational Science*, 62:101695, 2022.
- 636
- 637 Luis Müller, Mikhail Galkin, Christopher Morris, and Ladislav Rampásek. Attending to graph
638 transformers. *Transactions on Machine Learning Research*, 2024. ISSN 2835-8856.
- 639 Galileo Namata, Ben London, Lise Getoor, Bert Huang, and U Edu. Query-driven active surveying
640 for collective classification. In *10th international workshop on mining and learning with graphs*,
641 volume 8, pp. 1, 2012.
- 642
- 643 Erlin Pan and Zhao Kang. Beyond homophily: Reconstructing structure for graph-agnostic clustering.
644 In *International Conference on Machine Learning*, pp. 26868–26877. PMLR, 2023.
- 645 Adam Paszke, Sam Gross, Francisco Massa, Adam Lerer, James Bradbury, Gregory Chanan, Trevor
646 Killeen, Zeming Lin, Natalia Gimelshein, Luca Antiga, et al. Pytorch: An imperative style,
647 high-performance deep learning library. *Advances in neural information processing systems*, 32,
2019.

- 648 Hongbin Pei, Bingzhe Wei, Kevin Chen-Chuan Chang, Yu Lei, and Bo Yang. Geom-gcn: Geometric
649 graph convolutional networks. In *International Conference on Learning Representations*, 2019.
650
- 651 Oleg Platonov, Denis Kuznedelev, Michael Diskin, Artem Babenko, and Liudmila Prokhorenkova.
652 A critical look at the evaluation of gnns under heterophily: Are we really making progress? In
653 *International Conference on Learning Representations*, 2023.
654
- 655 Oleg Platonov, Denis Kuznedelev, Artem Babenko, and Liudmila Prokhorenkova. Characterizing
656 graph datasets for node classification: Homophily-heterophily dichotomy and beyond. *Advances
657 in Neural Information Processing Systems*, 36, 2024.
- 658 Hao Qian, Hongting Zhou, Qian Zhao, Hao Chen, Hongxiang Yao, Jingwei Wang, Ziqi Liu, Fei
659 Yu, Zhiqiang Zhang, and Jun Zhou. Mdgnn: Multi-relational dynamic graph neural network for
660 comprehensive and dynamic stock investment prediction. In *Proceedings of the AAAI Conference
661 on Artificial Intelligence*, volume 38, pp. 14642–14650, 2024.
- 662 Chenyang Qiu, Guoshun Nan, Tianyu Xiong, Wendi Deng, Di Wang, Zhiyang Teng, Lijuan Sun,
663 Qimei Cui, and Xiaofeng Tao. Refining latent homophilic structures over heterophilic graphs
664 for robust graph convolution networks. In *Proceedings of the AAAI Conference on Artificial
665 Intelligence*, volume 38, pp. 8930–8938, 2024.
666
- 667 Ladislav Rampásek, Michael Galkin, Vijay Prakash Dwivedi, Anh Tuan Luu, Guy Wolf, and Do-
668 minique Beaini. Recipe for a general, powerful, scalable graph transformer. *Advances in Neural
669 Information Processing Systems*, 35:14501–14515, 2022.
- 670 Prithviraj Sen, Galileo Namata, Mustafa Bilgic, Lise Getoor, Brian Galligher, and Tina Eliassi-Rad.
671 Collective classification in network data. *AI magazine*, 29(3):93–93, 2008.
672
- 673 Yunsheng Shi, Zhengjie Huang, Shikun Feng, Hui Zhong, Wenjin Wang, and Yu Sun. Masked label
674 prediction: Unified message passing model for semi-supervised classification. In *International
675 Joint Conference on Artificial Intelligence*, pp. 1548–1554, 2021.
- 676 Yunchong Song, Chenghu Zhou, Xinbing Wang, and Zhouhan Lin. Ordered gnn: Ordering message
677 passing to deal with heterophily and over-smoothing. In *The Eleventh International Conference on
678 Learning Representations*, 2023.
679
- 680 Victor Sreeram and P Agathoklis. On the properties of gram matrix. *IEEE Transactions on Circuits
681 and Systems I: Fundamental Theory and Applications*, 41(3):234–237, 1994.
- 682 Susheel Suresh, Vinith Budde, Jennifer Neville, Pan Li, and Jianzhu Ma. Breaking the limit of
683 graph neural networks by improving the assortativity of graphs with local mixing patterns. In
684 *Proceedings of the 27th ACM SIGKDD Conference on Knowledge Discovery & Data Mining*, pp.
685 1541–1551, 2021.
686
- 687 Laurens Van der Maaten and Geoffrey Hinton. Visualizing data using t-sne. *Journal of machine
688 learning research*, 9(11), 2008.
- 689 Petar Veličković, Guillem Cucurull, Arantxa Casanova, Adriana Romero, Pietro Liò, and Yoshua
690 Bengio. Graph attention networks. In *International Conference on Learning Representations*,
691 2018.
692
- 693 Daixin Wang, Zhiqiang Zhang, Yeyu Zhao, Kai Huang, Yulin Kang, and Jun Zhou. Financial default
694 prediction via motif-preserving graph neural network with curriculum learning. In *Proceedings of
695 the 29th ACM SIGKDD Conference on Knowledge Discovery and Data Mining*, pp. 2233–2242,
696 2023.
- 697 Minjie Wang, Da Zheng, Zihao Ye, Quan Gan, Mufei Li, Xiang Song, Jinjing Zhou, Chao Ma,
698 Lingfan Yu, Yu Gai, et al. Deep graph library: A graph-centric, highly-performant package for
699 graph neural networks. *arXiv preprint arXiv:1909.01315*, 2019.
700
- 701 Xiyuan Wang and Muhan Zhang. How powerful are spectral graph neural networks. In *International
Conference on Machine Learning*, pp. 23341–23362. PMLR, 2022.

- 702 Yu Wang and Tyler Derr. Tree decomposed graph neural network. In *Proceedings of the 30th ACM*
 703 *international conference on information & knowledge management*, pp. 2040–2049, 2021.
- 704
- 705 Yujie Xing, Xiao Wang, Yibo Li, Hai Huang, and Chuan Shi. Less is more: on the over-globalizing
 706 problem in graph transformers. In *Forty-first International Conference on Machine Learning*,
 707 2024.
- 708
- 709 Keyulu Xu, Chengtao Li, Yonglong Tian, Tomohiro Sonobe, Ken-ichi Kawarabayashi, and Stefanie
 710 Jegelka. Representation learning on graphs with jumping knowledge networks. In *International*
 711 *conference on machine learning*, pp. 5453–5462. PMLR, 2018.
- 712
- 713 Zhe Xu, Yuzhong Chen, Qinghai Zhou, Yuhang Wu, Menghai Pan, Hao Yang, and Hanghang Tong.
 714 Node classification beyond homophily: Towards a general solution. In *Proceedings of the 29th*
 715 *ACM SIGKDD Conference on Knowledge Discovery and Data Mining*, pp. 2862–2873, 2023.
- 716
- 717 Yujun Yan, Milad Hashemi, Kevin Swersky, Yaoqing Yang, and Danai Koutra. Two sides of the
 718 same coin: Heterophily and oversmoothing in graph convolutional neural networks. In *2022 IEEE*
International Conference on Data Mining (ICDM), pp. 1287–1292. IEEE, 2022.
- 719
- 720 Liang Yang, Mengzhe Li, Liyang Liu, Chuan Wang, Xiaochun Cao, Yuanfang Guo, et al. Diverse
 721 message passing for attribute with heterophily. *Advances in Neural Information Processing Systems*,
 722 34:4751–4763, 2021.
- 723
- 724 Yuhao Yang, Chao Huang, Lianghao Xia, Yuxuan Liang, Yanwei Yu, and Chenliang Li. Multi-
 725 behavior hypergraph-enhanced transformer for sequential recommendation. In *Proceedings of the*
 726 *28th ACM SIGKDD conference on knowledge discovery and data mining*, pp. 2263–2274, 2022.
- 727
- 728 Xinyi Zhang, Yanni Xu, Changzhi Jiang, Lian Shen, and Xiangrong Liu. Molemcl: a multi-level
 729 contrastive learning framework for molecular pre-training. *Bioinformatics*, 40(4):btac164, 2024.
- 730
- 731 Xin Zheng, Yixin Liu, Shirui Pan, Miao Zhang, Di Jin, and Philip S Yu. Graph neural networks for
 732 graphs with heterophily: A survey. *arXiv preprint arXiv:2202.07082*, 2022.
- 733
- 734 Jiong Zhu, Yujun Yan, Lingxiao Zhao, Mark Heimann, Leman Akoglu, and Danai Koutra. Beyond
 735 homophily in graph neural networks: Current limitations and effective designs. *Advances in neural*
 736 *information processing systems*, 33:7793–7804, 2020.
- 737
- 738 Jiong Zhu, Yujun Yan, Mark Heimann, Lingxiao Zhao, Leman Akoglu, and Danai Koutra. Heterophily
 739 and graph neural networks: Past, present and future. *IEEE Data Engineering Bulletin*, 2023.

739 A APPENDIX

741 A.1 PROOF OF THEROEMS

743 Firstly, we describe the formula derivation process of the l -layer GNN $\mathbf{X}^{(l)} =$
 744 $\prod_{i=1}^l \hat{\mathbf{A}}^{(l-i+1)} \mathbf{X}^{(0)} \mathbf{W}^{(i)}$. For simplicity, the $\sigma(\cdot)$ function (*i.e.*, *ReLU*) is omitted as mentioned
 745 before. Thus, for traditional GNNs,

$$\begin{aligned}
 746 \mathbf{X}^{(l)} &= \hat{\mathbf{A}}^{(l)} \mathbf{X}^{(l-1)} \mathbf{W}^{(l)} \\
 747 &= \hat{\mathbf{A}}^{(l)} (\hat{\mathbf{A}}^{(l-1)} \mathbf{X}^{(l-2)} \mathbf{W}^{(l-1)}) \mathbf{W}^{(l)} \\
 748 &\dots \\
 749 &= \prod_{i=1}^l \hat{\mathbf{A}}^{(l-i+1)} \mathbf{X}^{(0)} \prod_{i=1}^l \mathbf{W}^{(i)}.
 \end{aligned}$$

754 Then, we prove Theorem 1.

755 **Proof of Theorem 1.**

Table 3: Statistics of the node classification datasets.

	Actor	Roman	Amazon	Minesweeper	Tolokers	Cora	Citeseer	Pubmed
#Nodes	7,600	22,662	24,492	10,000	11,758	2,708	3,327	19,717
#Edges	26,659	32,927	93,050	39,402	519,000	5,278	4,552	44,324
#Features	931	300	300	7	10	1,433	3,703	500
#Classes	5	18	5	2	2	7	6	3
h_{edge}	0.22	0.05	0.38	0.68	0.59	0.81	0.74	0.80
LI	0.00	0.11	0.04	0.00	0.01	0.59	0.45	0.41

Proof 1 For traditional GNNs,

$$\mathbf{x}_i^{(l)} = \sigma\left(\sum_{j \in \mathcal{N}(i)} c_{ij} \mathbf{W} \mathbf{x}_j^{(l-1)}\right).$$

Here, c_{ij} is the weight coefficient of node j to node i . And for heterophilic graphs, $c_{ij} \leq 1$ and don't tend to 1.

The influence of a k -order neighbor i_k to node i_0 in the path \mathcal{P} is calculated as:

$$C_{i_0 i_k}^{\mathcal{P}} = \prod_{j=0}^{k-1} c_{i_j i_{j+1}}.$$

Thus, as k grows, the influence intensity $C_{i_0 i_k}^{\mathcal{P}}$ becomes smaller.

Therefore, we conclude that:

$$\lim_{k \rightarrow \infty} C_{i_0 i_k}^{\mathcal{P}} = 0.$$

A.2 DATASETS DETAILS

In this part, we describe three homophilic datasets and five heterophilic datasets and the heterophily metric of these datasets. The statistics for these datasets are presented in Table 3.

Homophilic Datasets: *Cora*, *CiteSeer*, and *PubMed* Namata et al. (2012); Kipf & Welling (2016) are datasets derived from citation networks. In these datasets, nodes symbolize papers, while edges denote citations between them, and the label of a node indicates the academic subject of the paper. These datasets are categorized as homophilic datasets.

Heterophilic Datasets: *Actor* Pei et al. (2019) is a subgraph where nodes denote actors and edges signify co-occurrences on a Wikipedia page. Node features are Wikipedia page keywords, and the aim is to classify nodes into five categories based on their page content. *Roman-empire* Lhoest et al. (2021); Platonov et al. (2023) challenges GNNs with low homophily, sparse links, and long-distance dependencies. In the dataset, nodes represent words and are connected if they are consecutive or syntactically related in a sentence. *Amazon-ratings* Leskovec & Krevl (2014); Platonov et al. (2023) is based on the Amazon product co-purchasing network metadata dataset from SNAP² Datasets. In the dataset, nodes are products, and edges connect products that are frequently bought together. The task is to predict the average rating given to a product by reviewers. *Minesweeper* Platonov et al. (2023) is a dataset based on the Minesweeper game. The graph is a 100x100 grid where each node connects to up to eight neighbors. The challenge is to identify the 20% of nodes randomly set as "mines". *Tolokers* Platonov et al. (2023) comprises nodes symbolizing tolokera (workers) who have been a part of one of 13 chosen projects³. The dataset aims to predict which tolokera faced bans in a project.

Heterophily Metric: There are two metrics we used to evaluate the heterophily of datasets. In general, h_{edge} has been the most often used metric, defined as:

²<https://snap.stanford.edu/data/amazon-meta.html>

³<https://github.com/Toloka/TolokerGraph>

$$h_{\text{edge}} = \frac{|(u, v) \in \mathcal{E} : y_u = y_v|}{|\mathcal{E}|}, \quad (11)$$

where y_u is the label of a node u and \mathcal{E} is the set of edges.

However, h_{edge} is not suitable for datasets with unbalanced classes. Then, the LI metric is introduced to address these shortcomings. LI quantifies how much information a neighbor’s label gives about the node’s label, making it more versatile in various graph scenarios. It is defined by:

$$LI = \frac{I(y_u, y_v)}{H(y_u)}, \quad (12)$$

where y_u and y_v are random labels of u and v respectively, $H(y_u)$ represents the entropy of y_u , and $I(y_u, y_v)$ denotes the mutual information between u and v .

A.3 DESCRIPTION OF BASELINE

In this part, we describe 18 baselines that we used to compare with our models. And descriptions are listed as follows:

(1) Deep learning method:

- **ResNet** He et al. (2016) is a deep learning model utilizing residual connections for effective deep network training. In graphs, it views nodes as independent samples, while ignoring the graph structure.

(2) Classic GNN methods:

- **GCN** Kipf & Welling (2016) is a semi-supervised graph convolutional network model that learns node representations by aggregating information from neighbors.
- **GraphSAGE** Hamilton et al. (2017) is a framework for inductive representation learning on large graphs based on sampling algorithms.
- **GAT** Veličković et al. (2018) uses attention mechanisms to weigh neighbor contributions, allowing different neighbors to contribute differently to the node’s new representation.
- **GATv2** Brody et al. (2022) improves upon GAT by introducing a more expressive and flexible dynamic attention mechanism.

(3) Selective information propagation methods:

- **H₂GCN** Zhu et al. (2020) integrates ego and neighbor-embedding separation, and higher-order neighborhoods, showing enhanced performance on heterophilic graphs.
- **GBK-GNN** Du et al. (2022) introduces a bi-kernel feature transformation, capturing both homophily and heterophily properties.
- **GCNII** Chen et al. (2020) is an extension of graph convolutional network with initial residual and identity mapping which can relieve the problem of over-smoothing.
- **FSGNN** Maurya et al. (2022) is a GNN model that uses “Soft-Selector” for adaptive feature choice and “Hop-Normalization” for improved node classification performance.
- **OrderedGNN** Song et al. (2023) is a GNN model that aligns the hierarchy of the rooted-tree of a central node with the ordered neurons in its node representation.

(4) Graph signal-based methods:

- **GPR-GNN** Chien et al. (2020) is a novel GNN architecture that adaptively learns Generalized PageRank (GPR) weights. It can effectively handle both homophily and heterophily and prevents feature over-smoothing.
- **FAGCN** Bo et al. (2021) utilizes a self-gating mechanism to adaptively integrate different signals in message passing, enhancing the adaptability of the model and addressing over-smoothing problems in various networks.

- **JacobiConv** Wang & Zhang (2022) is a spectral graph neural network approach that leverages Jacobi polynomial basis.
- **ALT-APPNP** Xu et al. (2023) is a structured-based method that decomposes a given graph and extracts complementary graph signals adaptively for node classification.

(5) Global information-based methods:

- **Graph Transformer (GT)** Shi et al. (2021) incorporates transformer architecture into GNNs. It uses self-attention mechanisms to capture global information in graph data.
- **GraphGPS** Rampášek et al. (2022) use self-attention mechanisms to capture global information while combining local message-passing and positional/structural encodings for improved scalability and performance.
- **GloGNN++** Li et al. (2022) introduce a global coefficient matrix to capture the correlations between nodes in each layer.
- **LRGNN** Liang et al. (2024) use a global label relationship matrix to replace the aggregation matrix by solving a robust low-rank matrix approximation problem.

A.4 TIME ANALYSIS

We compare our model with GAT and Graph Transformer (GT) in terms of training time for 1000 epochs across the five largest datasets. As shown in Table 4, GloMP-GNN consistently outperforms GT in training time, while striking an effective balance between the efficiency of GAT and the broader information aggregation of GT. GAT achieves the shortest training times due to its local attention mechanism, which focuses on neighboring nodes, but at the expense of capturing global relationships. GT incorporates more complex transformations and global attention, leading to longer training times.

Table 4: Training Time Comparison for 1000 Epochs on the Five Largest Datasets.

Model	Tolokers	Amazon	Minesweeper	Pubmed	Roman
GAT	41s	35s	23s	29s	32s
GT	68s	58s	32s	46s	53s
GloMP-GNN	43s	38s	27s	31s	34s

A.5 FURTHER EXPERIMENTS ON OVER-SMOOTHING

In order to quantify the ability of GloMP-GNN to mitigate over-smoothing problem, we compute the Dirichlet Energy of 64 layers for GloMP-GNN after training. As shown in Table 5, GloMP-GNN exhibits significantly higher Dirichlet Energy on the Actor, Minesweeper, and Cora datasets compared to GCN and GCNII. This indicates that GloMP-GNN better preserves the diversity of node features, making it more resistant to the over-smoothing problem.

Table 5: Dirichlet Energy of 64 layers for GloMP-GNN after training. The higher energy indicates that it is less prone to over-smoothing.

Model	Actor	Minesweeper	Cora
GCN	0.1633	0.0007	0.0791
GCNII	0.3155	0.4312	0.1562
GloMP-GNN	0.7176	0.5936	0.2782